The 2015 World Congress on
Aeronautics, Nano, Bio, Robotics, and Energy (ANBRE15)
Incheon, Korea, August 25-28, 2015

The Ultimate Flow Controlled Wind Turbine Blade Airfoil

Seifert Avraham[1)] Friedland Ori[2)] and Dolgopyat Danny[3)]

[1), 2), 3)] *School of Mechanical Engineering, Faculty of Engineering, Tel Aviv University*
Tel Aviv 69978, ISRAEL
[1)] *seifert@eng.tau.ac.il*

ABSTRACT

Active flow control (AFC) is being studied as an enabling technology that enhances and maintains high efficiency for wind turbine blades which can perform with contaminated surfaces, in unsteady winds, and at off-design operating conditions. The study is focused on a 25% thick airfoil (DU91-W2-250), which suitable because of the mid blade radius location. Initially a clean airfoil was fabricated, tested, and compared to XFoil predictions. From these experiments, the evolution of the separation location was identified. Five locations for installing active flow control actuators are available on this airfoil. It is intended to implement both Piezo fluidic ("Synthetic jets") and the Suction and Oscillatory Blowing (SaOB) actuators. Then it is planned to evaluate both actuation concepts' overall energy efficiency and efficacy in controlling boundary layer separation. Since efficient actuation is possible at low amplitudes when actuators are placed close to the separation location, distributed actuation is used. An array of hot-film and unsteady pressure sensors will enable real-time monitoring of the separation location and lift, respectively. After completing the baseline studies the study is now focused on the airfoil instrumentation with actuators and sensors. By the time of the conference, active flow control results will be available.

Introduction

In 2008 Johnson et al (Johnson 2008) reviewed the state of the art in flow control devices and techniques applicable for load and flow control over wind turbines. They concluded that out of the 15 techniques that were evaluated, many seemed appropriate for wind turbine load and flow control. Though they prefer devices that can modify the linear range of the lift curve, the opinion was that separation delay mechanisms should also be considered. In a more recent review (Pechlivanoglou 2011) the authors list the relevant AFC devices for wind turbine AFC and conclude that …

Synthetic jet (SJ hereafter) actuators (Glezer 2002) were among the devices discussed in (Johnson 2008, Pechlivanoglou 2011). These devices were shown in many instances (Troshin 2013, Yehoshua 2006 ,Timor 2007, Stalnov 2010) and as reviewed in Cattafesta (2011) to be both a viable and an efficient flow control device. However, the control authority of SJ actuators is somewhat limited and the requirement for high voltage excitation and multiple wiring requirements is considered a shortcoming of the robustness and long term reliability.

[1)] Professor

A new AFC device was introduced to the flow control community in 2004: the Suction and Oscillatory blowing actuator (Arwatz 2008). This no-moving-parts device can create two very effective flow control effectors (i.e., steady suction and sideways oscillating wall jets, in one embodiment) in close proximity to each other. The SaOB actuator has been demonstrated to be both robust and efficient in a range of studies and applications (Seifert 2008, Wilson 2013, Shtendel 2014).

As any other flow control method, AFC actuators require energy input. The purpose of the current study is therefore to compare the overall energy efficiency of SJA and the SaOB actuators as tools for the delay of boundary layer separation on wind turbine blades.

RESULTS

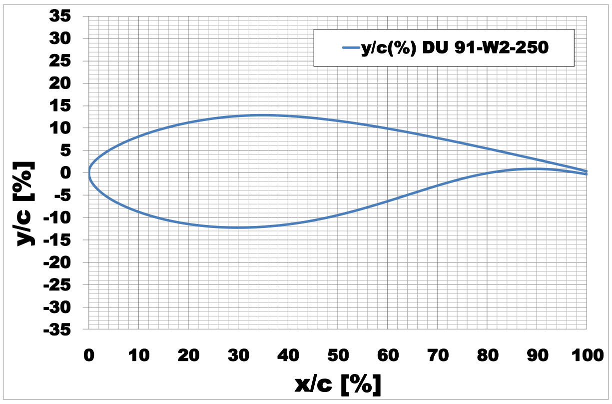

Fig. 1 The contour of the original DU91-W2-250 airfoil.

Fig. 2 The clean DU91-W2-250 airfoil, showing 3 of the 5 inserts where actuators will later be installed, in the Knapp-Meadow wind tunnel of Tel Aviv University. Chord c=480mm.

In Figure 1 we present the original contour of the DU91-W2-250 airfoil. The airfoil was fabricated from 3mm thick Fiberglass epoxy skin followed by a CNC made “negative”. A combination of wood and metal frames connects the airfoil to the turntables. About 100 pressure taps were installed around the airfoil, mainly over its upper surface.

In Figure 2 we present the airfoil with the inserts machined in 5 locations, which were covered and smoothed for minimal effect on laminar-turbulent boundary layer transition. Following airfoil installation, lift, drag and moments were calculated from measurements of airfoil pressures and wake velocity distributions. The wake velocity was extracted from total pressure ports, located about 2 chords downstream of the airfoil. The range of tested Reynolds numbers was 0.2 to 1.2×10^6. The integral results were compared to XFoil calculations and the results are presented in Figures 3-4.

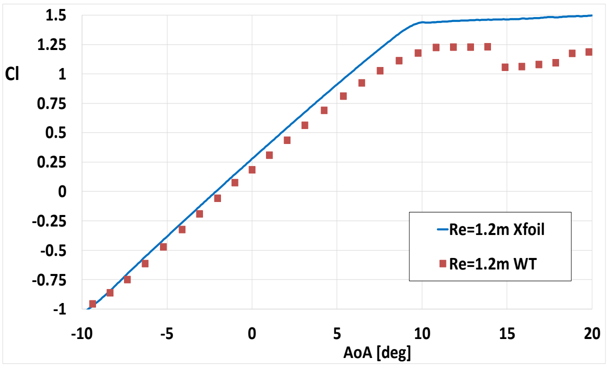

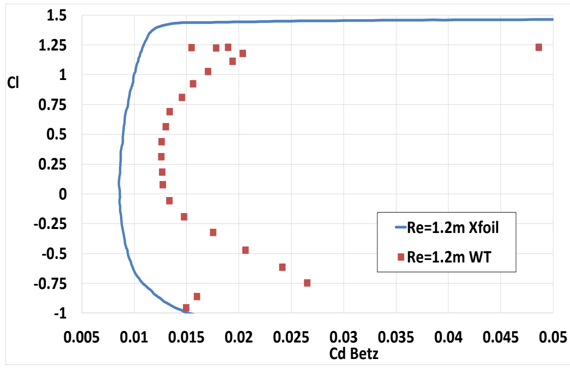

Fig. 3 Lift coefficient vs. incidence angle, Re=1.2x10^6, clean, original airfoil with no actuators, with slot-inserts.

Fig. 4 Lift coefficient vs. drag coefficient, Re=1.2x10^6, clean, original airfoil with no actuators, with slot-inserts.

In Figure 3 we present the lift coefficient from the experiment compared to the XFoil generated data at Re=1.2x10^6. The experimental lift slope is slightly lower than the calculated one, possibly related to the lack of wind tunnel corrections. The stall is mild in both experiment and predicted data. However, the experimental maximum lift is lower by about 0.2 compared to the XFoil predictions. One should note however, that natural transition was assumed in XFoil, while the slight discontinuities in the experimental model cannot simply be accounted for in this software. Overall the agreement in lift is reasonable, taking all the uncertainties into account.

The lift-drag polar is presented in Figure 4. The minimum drag is higher by about 0.005 and the drag diverges quicker than in the XFoil predictions. This effect can again be attributed to the actuator slot inserts that are not perfectly smooth as the software assumes. The reducing drag at the positive and negative stall regions is attributed to unsteady flow or to laminar separation with turbulent reattachment; in any event, these effects are associated to the specifics of the test and are not universal.

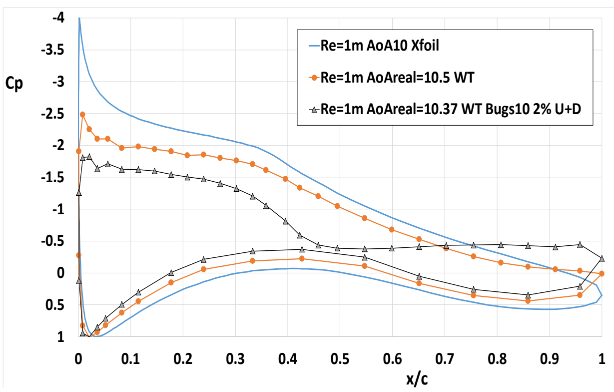

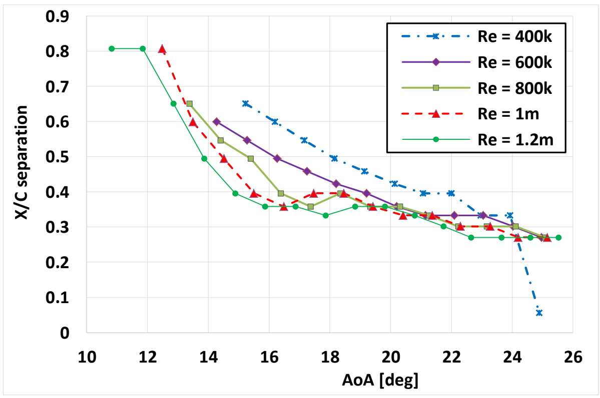

Fig. 5 Pressure distributions along the airfoil chord for clean and tripped conditions, AoA=10deg and Re=1.0x10^6.

Fig. 6 Boundary layer separation location based on the Cp plateau. Reynolds number in Legend, clean airfoil.

In order to examine the relevance of our actuator slot locations we consider now the pressure coefficient, Cp, distributions, from which we can extract the separation region and place AFC actuators upstream of the separation location.

In Figure 5 we present 3 Cp distributions at an incidence angle of 10 degrees and Reynolds number of one million. The XFoil data (blue line) is compared to the baseline-clean Cp (red circles) and in agreement with the lower experimental lift (by about 0.2, Fig. 3) the experimental Cp is less negative on the upper surface. However, the general trend of the pressure distributions is similar. The Cp indicates a nullifying trailing edge pressure for this condition. When “bugs” in the form of dots with diameter of 1.0 mm and height of 0.5 mm were placed on the upper and lower surface at x/c=0.02, every 10 mm in the span (y) direction, the boundary layers became turbulent further upstream, got thicker and lost more momentum. Therefore, premature trailing edge separation took place, as shown by the black triangles in Figure 5. The plateau in the Cp of the upper surface, from the trailing edge to x/c=0.35, indicates that separation occurred at this stream-wise location. Using the condition $\frac{\partial C_p}{\partial (x/c)} > -0.75$, separation is shown to initiate at the trailing edge at all Reynolds numbers (Figure 6) and moves forward until it is arrested in the range 0.25<x/c<0.35. Only at Re=0.4x10^6 does separation move forward all the way to the leading edge. It would be interesting to see how actuators placed at x/c=0.8, 0.6 and 0.4 would be capable of slowing down the forward motion of the separation line. As a result of the low probability of the separation line moving all the way to the leading edge, the x/c=0 slot location is not planned to be used in the 1st stage of the study and is left sealed and smooth as possible.

Following the baseline wind tunnel tests the airfoil was taken out of the tunnel, and four rows of actuators were installed. The 3 front rows (x/c=0.2, 0.4 and 0.6) included both Piezo fluidic “Synthetic jets” and SaOB actuators. At the x/c=0.8 slot, only Piezo fluidic actuators were placed, due to lack of internal space close to the trailing-edge. The SJAs are operated at their Helmholtz resonance frequency, and can also be amplitude or pulse modulated with any desired number of cycles to create low frequencies. The SaOB actuators are synchronized (each row) and also create suction

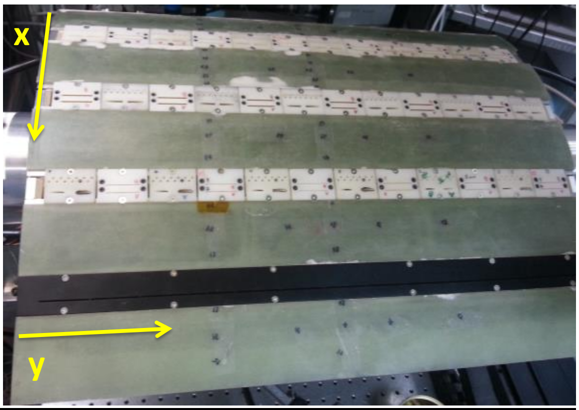

Fig. 8 The instrumented airfoil with 4 rows of AFC staggered actuators of two types. Actuator locations: x/c=0.2, 0.4, 0.6 and 0.8.

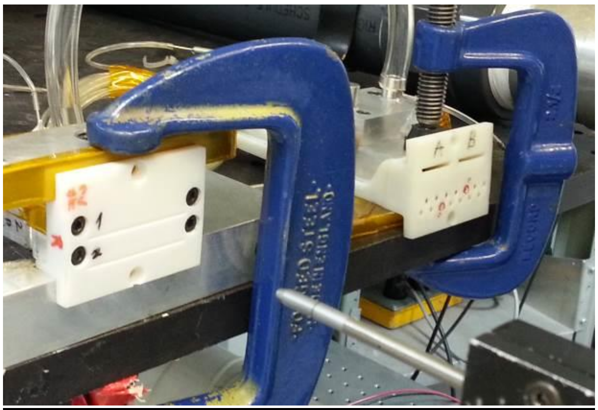

Fig. 7 The Suction and pulsed blowing actuator (right) with 3D “printed” housing and the SJA (left) ready to be calibrated.

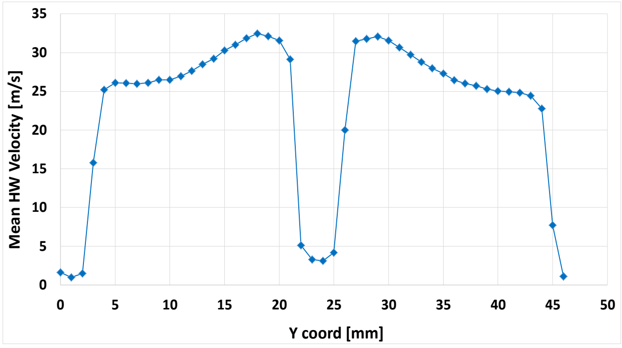

Fig. 9 Mean velocity distribution along the pulsed blowing slot of the SaOB actuator.

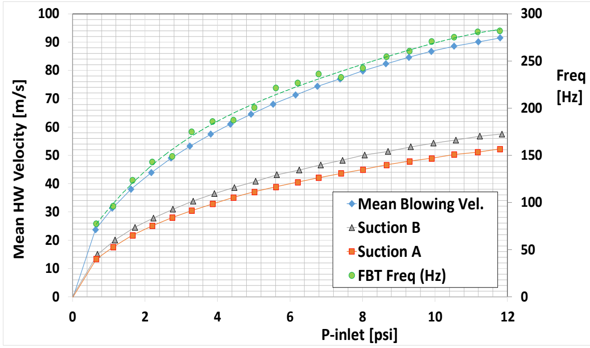

Fig. 10 Typical SaOB actuator performance vs. Inlet pressure, showing mean pulsed blowing velocity, suction velocities and frequency (with right side ordinate)

through two staggered rows of suction holes for each actuator. See Figure 8. The actuators were each calibrated on a dedicated bench-top set-up prior to installation, as shown in Figure 7. The actuator operation was also validated as installed.

Typical bench-top results of the SaOB actuator performance are presented in Figure 9 and in Figure 10. In Figure 9 we see a scan along one pair of pulsed blowing slots connected to one SaOB actuator. Note there is effective actuation over about 45 mm of span with quite a uniform spread of the oscillatory wall jet to the sides. In Figure 10 we can observe the mean pulsed blowing velocity, the suction velocity of two suction holes and the oscillation frequency versus the inlet pressure. It is shown that all parameters are related to the inlet pressure. The suction velocity is roughly half the mean pulsed blowing velocity. Also of interest is the high efficiency of the actuator for inlet pressures below 2psi and decreasing efficiency for elevated inlet pressure. A mean velocity of 90m/s is easily achieved.

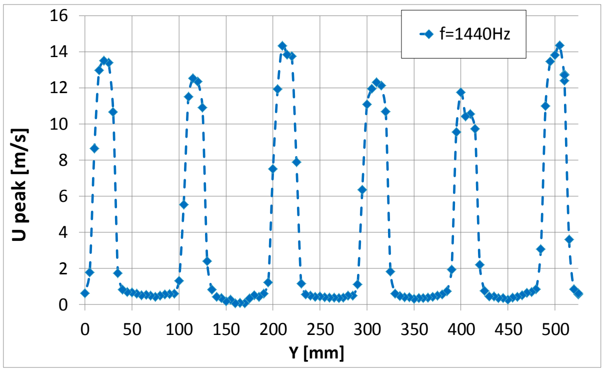

Fig. 11 Mean SJA velocity measured 10mm from the slot. Excitation voltage 60 Vrms.

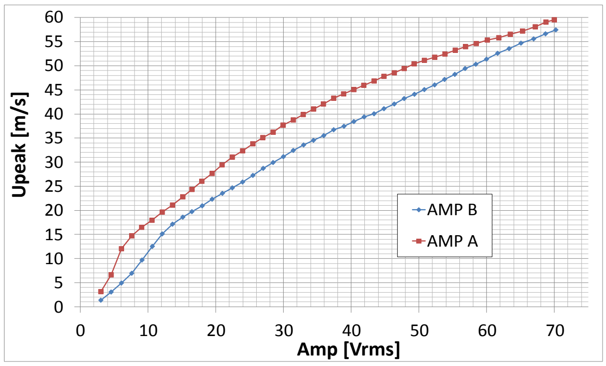

Fig. 12 An amplitude scan of the Piezo actuators at 1500Hz, Peak cycle velocity shown. Bench top tests.

In Figures 11 and 12 we present sample performance of the Piezo fluidic actuators. Figure 11 presents the mean pulsed blowing velocity across the 46mm long slot. This data was measured 10mm from the slot, such that the entrainment process has decreases the fluctuations and increases the mean velocity (from its mean of zero at the slot). The data in Figure 11 can be used to evaluate the level of uniformity across the span of the airfoil when 6 Piezo fluidic SJA's are being operated. Also note the shrinking of the resulting jet in the Y direction, due to axis switching.

Figure 12 presents an amplitude scan of the two slots of a single Piezo fluidic actuator. These actuators are operated at their Helmholtz resonance frequency of about 1500hz. It can be seen that the response is proportional to the excitation voltage, and peak velocities on the order of 60m/s are easily achievable. The phase and amplitude of each Piezo fluidic actuator is computer controlled. These performance of both actuation concepts assure sufficient control authority and warrant the tunnel entry.

Conclusions and Outlook

This paper describes the most comprehensive active flow control effort to date applied to boundary layer separation control on a wind turbine airfoil. Two leading actuation concept candidate technologies are implemented, i.e., Piezo fluidic “Synthetic jets” and the Suction and Pulsed Blowing (SaOB) actuators. Four rows of actuators in staggered configuration are installed between the 20% and 80% chord locations, where the initially trailing edge boundary layer separation progresses upstream as the airfoil stalls. The performance goals of the actuators were met and the instrumented airfoil is ready to be tested. By the time of the conference active flow control results will be available.

REFERENCES

Arwatz, G., Fono, I. and Seifert, A. (2008), "Suction and Oscillatory Blowing Actuator Modeling and Validation", AIAA J., V. 40, N. 5, pp. 1007-1017.

Cattafesta , L.N. III and Sheplak, M. (2011), "Actuators for active flow control", Annual Review of Fluid Mechanics.

Glezer, A. and Amitay, M. (2002), "Synthetic jets", Annual Review of Fluid Mechanics.

Johnson, S.J., van Dam, C.P. and Berg, D.E. (2008), “Active Load Control Techniques for Wind Turbines”, Sandia Report SAND2008-4809.

Pechlivanoglou, G., Nayeri, C. N. and Paschereit, C. O. (2011), “Performance Optimization of Wind Turbine Rotors With Active Flow Control”, Paper No. GT2011-45493, pp. 763-775; doi:10.1115/GT2011-45493.

Seifert, A. et al, (2008), “Heavy trucks drag reduction by active flow control”, AIAA paper 2008-0743, Jan.

Stalnov, O, Kribus A. and Seifert A. (2010), "Evaluation of active flow control applied to wind turbine blade section", AIP J. of Sustainable and Renewable Energy, 2, 063101 (2010); doi:10.1063/1.3518467, October 2010.

Shtendel, T. and Seifert, A. (2014), “Three-dimensional Aspects of bluff-body drag reduction by active flow control”, Int. J. Heat and Flow, V. 45, Pp 109–12.

Timor, I., Ben-Hamou, E., Guy, Y. and Seifert, A. (2007), “Maneuvering Aspects and 3D Effects of Active Airfoil Flow Control”, (prev. AIAA paper 2004-2614), Flow, Turb. and Comb. 78: 429-443.

Troshin, V. and Seifert, A. (2013), “High-performance Wind Turbine Airfoil using Distributed Closed-loop Flow Control System”, Experiments in Fluids 54:1443.

Wilson, J., Schatzmann, D., Arad, A., Seifert, A. and Shtendel, T. (2013), “Suction and Pulsed-Blowing Flow Control Applied to an Axisymmetric Body”, AIAA J.: 1-15 1.

Yehoshua, T. and Seifert, A. (2006), “Active boundary layer tripping using oscillatory vorticity generator”, Aerospace Science and Technology, 10 (3): 175-180.